

# A New Object-Weighted Measure of the Small-Scale Velocity Dispersion

Jonathan E. Baker and Marc Davis

*Astronomy Department, University of California, Berkeley, CA 94720*

**Abstract.** We describe a new statistic for measuring the small-scale velocity dispersion of galaxies directly from redshift surveys. This statistic is based on the object-weighted statistic proposed by Davis, Miller, & White (1997). Compared with the traditional pair-weighted velocity dispersion, our statistic is less sensitive to the presence or absence of rare, rich clusters of galaxies. This measure of the thermal energy of the galaxy distribution is ideally suited for use with a filtered version of the cosmic energy equation. We discuss the application of the statistic to the Las Campanas Redshift Survey. The low observed dispersion strongly favors cosmological models with low matter density,  $\Omega_m \sim 0.2$ .

## 1. Introduction

Redshift surveys provide an accurate measure of the Hubble recession velocity  $H_0 r$  plus radial peculiar velocity (relative to the velocity  $\mathbf{v}_0$  of the observer):

$$cz = H_0 r + (\mathbf{v}_{\text{pec}} - \mathbf{v}_0) \cdot \hat{\mathbf{r}} \quad (1)$$

for large samples of galaxies. In the gravitational instability paradigm for structure formation, peculiar velocities grow in response to the total (not just visible) amount of clustered mass. Measurements of the magnitude of these peculiar velocities are an important cosmological probe, with the potential to discriminate cosmological models, to constrain the bias of the galaxy distribution, and to constrain models for structure formation.

On relatively large (few Mpc and up) scales, peculiar velocities define a smooth flow field, the divergence of which is simply given by the galaxy overdensity times the parameter  $\beta \approx \Omega_m^{0.6}/b$ , where  $b = \delta_g/\delta_m$  is the galaxy bias. A number of methods have been devised for combining redshift and peculiar velocity surveys to obtain  $\beta$  from these large-scale flows (Strauss, this volume; Willick, this volume). These methods have not fully converged to a consistent solution; while POTENT prefers  $\beta \sim 1$  (e.g., Sigad et al. 1998), other methods tend to give low values  $\beta \approx 0.5$  (e.g., Willick & Strauss 1998).

Turning to small scales of order 1 Mpc, we find that peculiar velocities are essentially thermal or incoherent. The kinetic energy contained in these motions can be used with a filtered version of the cosmic energy equation to yield an estimate of  $\Omega_m/b^2$ , which is approximately equal to  $\beta^2$ .

It has been known for some time that the thermal energy of the galaxy distribution is quite low, or equivalently the cosmic Mach number is rather high,

relative to our theoretical expectations. A simple way to see this is to take an  $N$ -body simulation and plot what it would look like in redshift space. In a box of length  $5000 \text{ km s}^{-1}$ , one sees very prominent, long “fingers of god”, which tend to wash out the collapsed filamentary structures typical of real redshift surveys. The flow in the vicinity of the Local Group has also been measured to be remarkably cold, with a dispersion of only  $60 \text{ km s}^{-1}$ , and no blue-shifted galaxies are seen outside the Local Group (Schlegel, Davis, & Summers 1994). Governato et al. (1997) showed that this is extremely hard to reproduce even in low- $\Omega_m$   $N$ -body simulations.

The pair velocity dispersion ( $\sigma_{12}$ ) is the traditional measure of small-scale velocities. Redshift surveys provide a set  $\{r_p, \pi\}$  of projected and radial separations in redshift space;  $\sigma_{12}$  can be estimated directly from the redshift-space correlation function  $\xi_z(r_p, \pi)$ , which is a convolution of the real-space correlation function  $\xi(r)$  with the pair velocity distribution function  $f(v)$  (the rms of which is  $\sigma_{12}$ ). An exponential  $f(v)$  has been found to fit well and is also expected from theoretical considerations.

The  $\sigma_{12}$  statistic was first applied to the CfA redshift survey by Davis & Peebles (1983), who measured  $340 \text{ km s}^{-1}$  at  $1h^{-1} \text{ Mpc}$  scales. The fact that this dispersion was much lower than that of the  $\Omega_m = 1$  simulations of Davis et al. (1985) was the original motivation for bias in the galaxy distribution. Gelb & Bertschinger (1994) later showed that no normalization of the standard Cold Dark Matter (SCDM) model could simultaneously match both the observed correlation amplitude and velocity dispersion. However, many authors pointed out that the pair statistic was not robust (e.g., Mo, Jing, & Borner 1993; Zurek et al. 1994; Somerville, Primack, & Nolthenius 1997; Guzzo et al. 1997; Jing, Mo, & Borner 1998). In particular, its pair-wise weighting makes  $\sigma_{12}$  very sensitive to the presence or absence of rare, rich clusters in the survey volume; the treatment of a few objects can greatly affect the result. The mean streaming motions of galaxies were also shown to have a considerable effect on the measured value of the dispersion.

In this work, we present the application of a new, object-weighted statistic to the Las Campanas Redshift Survey (LCRS; Shectman et al. 1996). The LCRS is the largest existing redshift survey which is nearly fully sampled. It contains 26,418 galaxies with a median redshift of approximately  $30,000 \text{ km s}^{-1}$ . The survey consists of six  $1.5^\circ \times 80^\circ$  slices (three at northern declinations and three in the south), and contains about 30 clusters.

Even with such a large and well-sampled survey as the LCRS, the measurement of the pair dispersion  $\sigma_{12}$  has been fraught with controversy. Fourier techniques (Landy, Szalay, & Broadhurst 1998) gave a low dispersion consistent with the old CfA value, but Jing & Borner (1998) showed that accounting for mean streaming motions increased the value to  $570 \pm 80 \text{ km s}^{-1}$ . Jing et al. (1998) found that simulations with  $\Omega_m h \sim 0.2$  could reproduce the observed pair dispersion, but they required a somewhat mysterious anti-bias in the galaxy distribution (i.e., higher mass-to-light ratios in dense regions).

Given the difficulty of reliably estimating the pair dispersion, it is clearly of interest to develop alternative statistics. Our statistic, called  $\sigma_1$ , is a modified version of the object-weighted statistic developed by Davis, Miller, & White (1997, hereafter DMW). We note that other alternatives to  $\sigma_{12}$  have been sug-

gested. Nolthenius & White (1987) proposed the mean dispersion of groups of galaxies; our statistic has the advantage that it does not require assigning galaxies to groups and averaging over the internal motions. The pair dispersion can also be measured as a function of local density (Kepner, Summers, & Strauss 1997; Strauss, Ostriker, & Cen 1998), but unlike  $\sigma_1$ , this must be computed in volume-limited samples. This work discusses the application of  $\sigma_1$  to the LCRS; a more complete description of our results may be found elsewhere (Baker, Davis, & Lin 1999).

## 2. The $\sigma_1$ Statistic

We start from the definition of the single-particle object-weighted dispersion proposed by DMW. These authors applied this statistic to the UGC and *IRAS* 1.2-Jy redshift surveys, which are much smaller than the LCRS survey. For the UGC catalog, they measured  $\sigma_1 = 130 \pm 15 \text{ km s}^{-1}$ , much colder than their  $\Omega_m = 1$   $N$ -body simulation, even when the simulation velocities were artificially cooled by a factor of two.

### 2.1. Definition of $\sigma_1$

Around each survey galaxy  $i$  in redshift space, we place a cylinder of radius  $r_p$  and half-length  $v_l$ , with the axis of symmetry along the redshift (radial) coordinate. All the galaxies which fall within the cylinder are considered to be neighbors of galaxy  $i$ . We typically take  $r_p = 1h^{-1} \text{ Mpc}$  and  $v_l = 2500 \text{ km s}^{-1}$ . We construct a histogram of the number of neighbor galaxies  $P_i(\Delta v)$  in bins of velocity separation  $\Delta v$ . We subtract the background distribution  $B_i(\Delta v)$  expected for an uncorrelated galaxy distribution, and then average over the  $N_g$  galaxies to obtain the final distribution:

$$D(\Delta v) = \frac{1}{N_g} \sum_i w_i [P_i(\Delta v) - B_i(\Delta v)], \quad (2)$$

where the weight for galaxy  $i$  is denoted by  $w_i$ .

In the original DMW formulation, the weight for each galaxy was simply given by its total number of neighbors in excess of background:

$$w_i^{-1} = \sum_{\Delta v} [P_i(\Delta v) - B_i(\Delta v)]. \quad (3)$$

It is this factor which gives the statistic its essential object weighting, in contrast to the traditional pair-weighted dispersion. However, galaxies with fewer neighbors than the background had to be deleted from consideration, which biased the statistic towards higher density (and thus hotter) objects.

We avoid the bias inherent in the original statistic by assigning  $w_i = 1$  for galaxies with less than one excess neighbor. In order to combine the high- and low-density galaxies sensibly, it is necessary to tabulate their distributions separately. We subtract off the tails of the distributions (within  $500 \text{ km s}^{-1}$  of  $v_l$ ) and then normalize each distribution so that the sum  $\sum_{\Delta v} D(\Delta v)$  is proportional to the number of galaxies included. This allows the high- and low-density

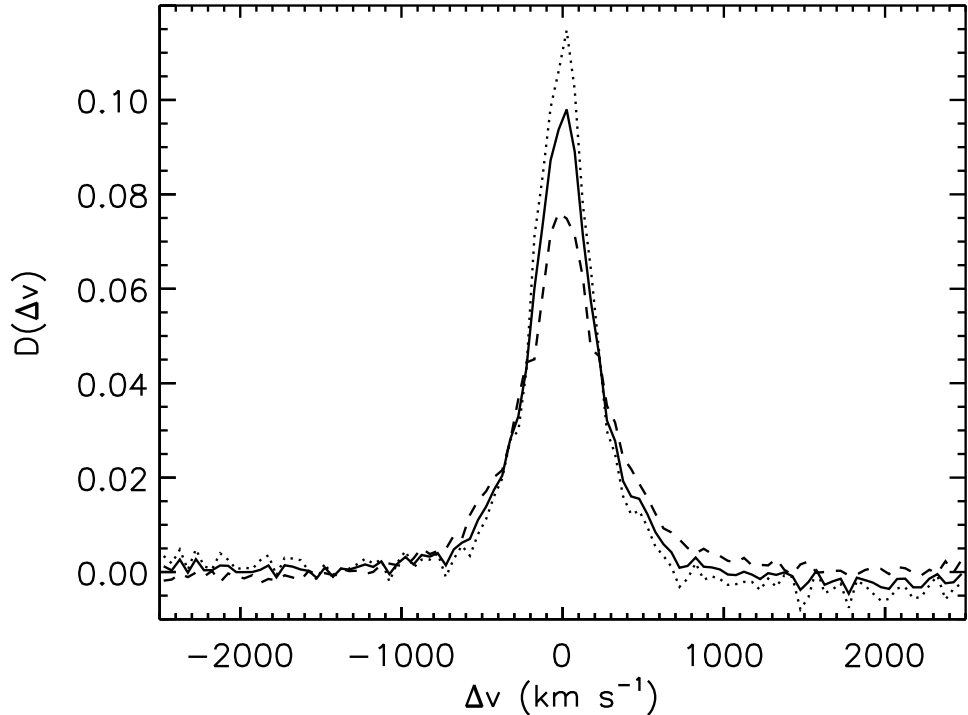


Figure 1. Object-weighted velocity distributions for the LCRS. We show distributions for galaxies in low-density (dashed) and high-density (dotted) regions, and the combined distribution (solid). The widths are  $\sigma_1 = 99, 207$ , and  $126 \text{ km s}^{-1}$ , respectively.

distributions to be combined so that they are weighted according to the number of objects assigned to them (see Figure 1).

We measure the width  $\sigma_1$  of the resulting distribution by performing a  $\chi^2$  fit to a model

$$M(\Delta v) = \overline{\xi_R} * f * E. \quad (4)$$

Here  $\overline{\xi_R}$  is the two-point correlation function  $\xi(r)$  averaged in the cylindrical bins,  $f \propto e^{-|v|/\sigma_1}$  is the velocity distribution function, and  $E$  is the error distribution of the redshift measurements (for the LCRS, a Gaussian of rms  $67 \text{ km s}^{-1}$ ). We find that the exponential form for  $f$  fits much better than a Gaussian for both the data and  $N$ -body simulations. We have defined  $\sigma_1$  so that it is a measure of the one-dimensional dispersion of the motion of individual galaxies, with bulk flows filtered out on scales larger than  $1h^{-1} \text{ Mpc}$ . We note that the rms of the distribution  $f$  is  $\sigma_1\sqrt{2}$ , which DMW distinguished from  $\sigma_1$  by calling it  $\sigma_I$ .

## 2.2. Cosmic Energy Equation

The cosmic energy, or Layzer-Irvine, equation is a differential relation between the kinetic and potential energies of the mass fluctuations in an expanding universe. It has been shown that for self-similar cosmological clustering, the

equation reduces to an algebraic expression:  $\langle v_{\text{pec}}^2 \rangle \approx g\Omega_m H_0^2 J_2$ , where  $J_2 \equiv \int r\xi(r) dr$  measures the potential energy and  $g \approx 0.3$ .

The difficulty in applying this equation to measure the mass density arises because the kinetic energy term and  $J_2$  are very poorly constrained on large scales. We therefore consider a filtered version of the equation, including contributions only from small scales. The simulations of DMW showed that  $\sigma_1$  is a good measure of the small-scale kinetic energy and can be used to estimate  $\Omega_m/b^2$  (the factor of  $b^2$  arises because we can only measure  $J_2$  for the galaxies rather than the underlying mass).

### 2.3. *N*-body Simulations

We have completed several cluster-normalized *N*-body simulations for comparison with the LCRS. The cosmological parameters of our models are given by Baker et al. (1999). They include a standard  $\Omega_m = 1$  (SCDM) model, a tilted variant with  $n = 0.8$  (TCDM), a flat model with a cosmological constant  $\Omega_\Lambda = 0.7$  (LCDM), and an open model with  $\Omega_m = 0.3$  (OCDM).

The models were evolved using a P3M code (Brieu, Summers, & Ostriker 1995) and a special-purpose GRAPE-3AF board (Okumura et al. 1993), which is hardwired to compute the Plummer force law very quickly. The board is attached to a Sun SPARC workstation which computes the long-range contributions to the forces. We are able to complete one cosmological run with  $64^3$  particles on a  $128^3$  mesh in approximately one CPU-day. Our box size is  $L = 50h^{-1}$  Mpc to match the length of the redshift-space cylinders used in the  $\sigma_1$  analysis.

We apply the same statistical procedure for computing  $\sigma_1$  for the LCRS to the particles in the simulations. Of course, galaxies may in general have a different velocity dispersion from the underlying mass, and the problem of identifying “galaxies” in the simulations is therefore an important one.

We first apply the standard friends-of-friends algorithm for defining halos, with a linking length of 0.2 mesh cells. With our relatively poor mass resolution, this procedure leads to a serious and well-known over-merging problem, yielding halo correlation functions which are much too low on small scales. To remedy this situation, we subdivide large ( $N > N_s$ ) halos by drawing individual particles from them at random, with a probability  $\propto N^{-\alpha}$ . For  $\alpha > 0$ , this yields a mass-to-light ratio which increases at small scales; this is required because  $\alpha = 0$  leads to correlation functions which are too steep in many models.

We choose the parameters  $\alpha$  and  $N_s$  to yield “galaxies” which match the correlation function and number density of the LCRS (about 2500 per simulation volume). We find that  $\alpha \sim 0.25$  is typically the best choice, and  $N_s \sim 80$ , corresponding to a mass of  $10^{13}\Omega_m h^{-1} M_\odot$ . Although by selecting individual particles as galaxies we are including the internal dispersions of galaxies, these velocities are small compared to the dispersions of the large clusters which are split. We have also measured  $\sigma_1$  for galaxies drawn from a large Virgo simulation (Benson et al. 1999) using semi-analytic techniques, and we find results consistent with our simulations.

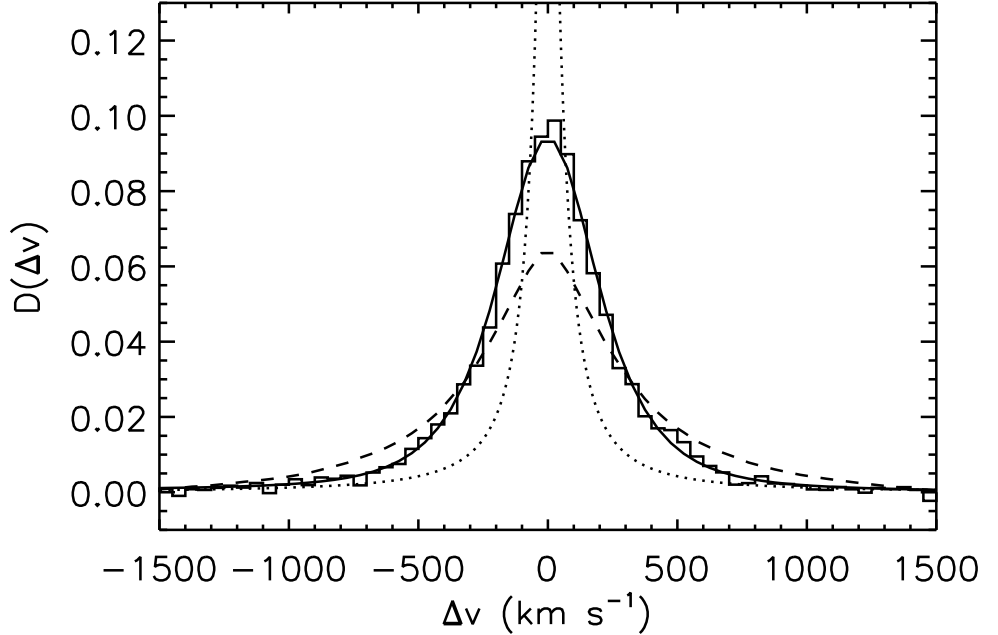


Figure 2. Velocity distributions for the LCRS data (histogram) and best-fitting model (solid curve) with  $\sigma_1 = 126 \text{ km s}^{-1}$ . Also shown are a model with no broadening ( $\sigma_1 = 0$ ; dotted) and the distribution for the mass in our SCDM simulation ( $\sigma_1 = 310 \text{ km s}^{-1}$ ; dashed).

### 3. Results

Based on the mean of the six LCRS slices, we measure  $\sigma_1 = 126 \pm 10 \text{ km s}^{-1}$ , where the quoted error is the standard deviation of the mean for the slices. The statistic is quite robust, with similar  $D(\Delta v)$  distributions for each of the slices. The fit is quite good, with  $\chi^2_\nu = 117/96 = 1.22$ , where we have estimated the errors from the standard deviation of the six slices. The distribution is plotted in Figure 2.

The exponential model also provides an excellent fit to the  $D(\Delta v)$  distributions in the simulations. We find that the mass in the SCDM and TCDM models is much too hot, with dispersions of over  $300 \text{ km s}^{-1}$ . The LCDM and OCDM models yield lower dispersions  $\sim 200 \text{ km s}^{-1}$ ; the OCDM model is slightly hotter than the LCDM. The halos are somewhat cooler, with velocity biases in the range 0.7–0.9. The LCDM halos are the best match to the LCRS dispersion, with  $\sigma_1 = 143 \text{ km s}^{-1}$ .

Combining the LCRS and  $N$ -body halo results, we can solve the cosmic energy equation for  $\Omega_m$  (the bias factor drops out because we have chosen halos which match the LCRS correlation function). We obtain similar results from each of the four cosmological models, with  $\Omega_m$  in the range 0.15–0.25. If we combine the LCRS and  $N$ -body mass, we obtain  $\Omega_m^{0.5}/b$ , approximately equal to

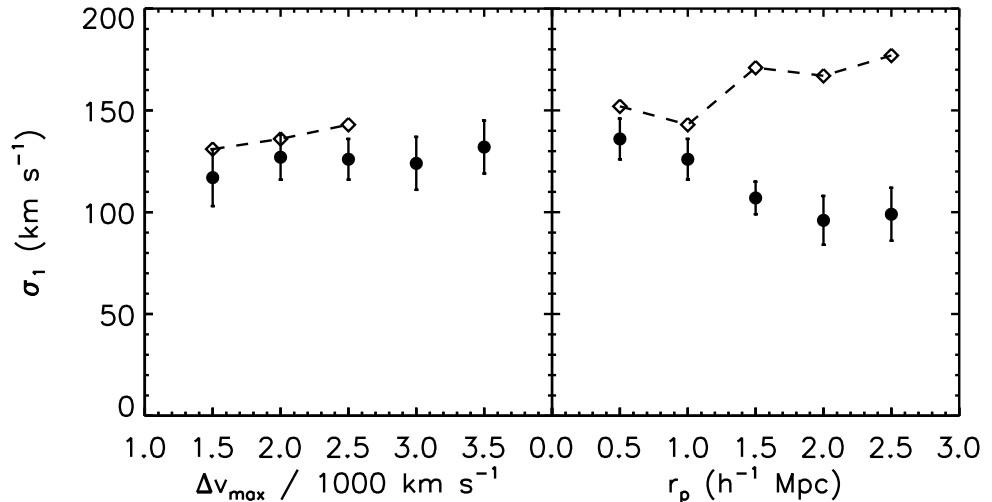


Figure 3. Dependence of  $\sigma_1$  on the cylinder length and radius. Filled points with error bars are for the LCRS, open points and dashed line are for galaxies in our LCDM simulation.

$\beta$ . The result is 0.3–0.4 for the two high-density models, and 0.4–0.6 for the two low-density models.

As we increase the radius  $r_p$  of the cylinders used to measure  $\sigma_1$ , we find an interesting discrepancy between the models and the LCRS data (Figure 3). The LCRS  $\sigma_1$  decreases modestly as the scale is increased, but all of the models show an increase with scale. It is at present unclear whether this discrepancy is a numerical artifact of the simulations or a real physical effect.

#### 4. Conclusions

We have applied a new object-weighted, unbiased measure of the small-scale velocity dispersion to the Las Campanas Redshift Survey. We derive a single-particle dispersion  $\sigma_1 = 126 \pm 10 \text{ km s}^{-1}$ . Our statistic has considerable advantages over the traditional pair dispersion  $\sigma_{12}$ ; namely, it is less sensitive to rare, rich clusters of galaxies. Our statistic should play an important role in analyses of future redshift surveys.

When compared with the LCRS data, cluster-normalized  $\Omega_m = 1$   $N$ -body simulations are far too hot on small scales. We find strong evidence for a low density  $\Omega_m \sim 0.2$ , and we derive consistent values of the density parameter from a number of different models; these results are described more fully elsewhere (Baker et al. 1999). In addition to constraining the mass density, the  $\sigma_1$  statistic applied to upcoming surveys should provide important constraints on the galaxy bias and evolution of structure.

**Acknowledgments.** We would like to thank S. Corneau for organizing a tremendously successful and enjoyable conference in Victoria, with an abundance

of Nanaimo bars which were consumed rapidly by at least one of the authors. J. E. B. acknowledges the support of an NSF graduate fellowship. This work was also supported in part by NSF grant AST95-28340.

## References

- Baker, J. E., Davis, M., & Lin, H. 1999, ApJ, submitted (astro-ph/9909030)
- Benson, A. J., Cole, S., Frenk, C. S., Baugh, C. M., & Lacey, C. G. 1999, MNRAS, submitted (astro-ph/9903343)
- Briau, P. P., Summers, F. J., & Ostriker, J. P. 1995, ApJ, 453, 566
- Davis, M., Efstathiou, G., Frenk, C. S., & White, S. D. M. 1985, ApJ, 292, 371
- Davis, M., Miller, A., & White, S. D. M. 1997, ApJ, 490, 63 (DMW)
- Davis, M. & Peebles, P. J. E. 1983, ApJ, 267, 465
- Gelb, J. M. & Bertschinger, E. 1994, ApJ, 436, 491
- Governato, F., Moore, B., Cen, R., Stadel, J., Lake, G., & Quinn, T. 1997, New Astronomy, 2, 91
- Guzzo, L., Strauss, M. A., Fisher, K. B., Giovanelli, R., & Haynes, M. P. 1997, ApJ, 489, 37 (astro-ph/9612007)
- Jing, Y. P. & Borner, G. 1998, ApJ, 503, 502
- Jing, Y. P., Mo, H. J., & Borner, G. 1998, ApJ, 494, 1
- Kepner, J. V., Summers, F. J., & Strauss, M. A. 1997, New Astronomy, 2, 165
- Landy, S. D., Szalay, A. S., & Broadhurst, T. J. 1998, ApJ, 494, L133
- Mo, H. J., Jing, Y. P., & Borner, G. 1993, MNRAS, 264, 825
- Nolthenius, R. & White, S. D. M. 1987, MNRAS, 225, 505
- Okumura, S. K., Makino, J., Ebisuzaki, T., Fukushige, T., Ito, T., Sugimoto, D., Hashimoto, E., Tomida, K., et al. 1993, PASJ, 45, 329
- Schlegel, D., Davis, M., & Summers, F. J. 1994, ApJ, 427, 527
- Shectman, S. A., Landy, S. D., Oemler, A., Tucker, D. L., Lin, H., Kirshner, R. P., & Schechter, P. L. 1996, ApJ, 470, 172
- Sigad, Y., Eldar, A., Dekel, A., Strauss, M. A., & Yahil, A. 1998, ApJ, 495, 516
- Somerville, R. S., Primack, J. R., & Nolthenius, R. 1997, ApJ, 479, 606
- Strauss, M. A., Ostriker, J. P., & Cen, R. 1998, ApJ, 494, 20
- Willick, J. A. & Strauss, M. A. 1998, ApJ, 507, 64
- Zurek, W. H., Quinn, P. J., Salmon, J. K., & Warren, M. S. 1994, ApJ, 431, 559